

Synthesis, characterization, and catalytic activity of nitrogen and iron(III) co-doped TiO₂

Patsaya Songkhum · Jonggol Tantirungrotechai

Received: 11 February 2011 / Accepted: 5 August 2011 / Published online: 13 June 2012
© Springer Science+Business Media B.V. 2012

Abstract The nitrogen and iron(III) co-doped TiO₂ (N–Fe–TiO₂) samples were synthesized via modified sol–gel method by using alkyl amine as both nitrogen source and pore directing agent. Morphologies and properties of the co-doped TiO₂ samples were investigated by X-ray diffraction, Fourier transform infrared spectroscopy, electron spin resonance spectroscopy, UV–Vis spectroscopy, scanning electron microscopy, and transmission electron microscopy. The results showed anatase phase mixed with rutile structure as well as hydroxyl and amine functional groups. The presence of Fe³⁺ in N–Fe–TiO₂ sample was detected at *g* value of 2.00. In addition, the prepared samples were photocatalytically active for methyl orange degradation under UV light irradiation, but not under visible light.

Keywords Co-doped TiO₂ · Sol–gel · Photocatalysis · Methyl orange dye

Introduction

Semiconductor photocatalysis has attracted much interest in recent years as an alternative for treating water polluted with hazardous chemicals. Titanium dioxide (TiO₂) has emerged as the most widely investigated photocatalyst because of its chemical stability, non-toxicity, inexpensive price, and well-positioned valence and

P. Songkhum
Materials Science and Engineering Program, Multi-Disciplinary Unit, Faculty of Science,
Mahidol University, Rama VI Rd., Bangkok 10400, Thailand
e-mail: psongkhum@gmail.com

P. Songkhum · J. Tantirungrotechai (✉)
Center for Catalysis, Department of Chemistry and Center of Excellence for Innovation
in Chemistry, Faculty of Science, Mahidol University, Rama VI Rd., Bangkok 10400, Thailand
e-mail: scjpp@mahidol.ac.th

conduction bands. It not only facilitates photodegradation of organic pollutants by UV light but also restrains some pathological activities. Thus, it is popular for application in wastewater treatment [1].

Although conventional semiconductors have revealed outstanding properties in photocatalysis, their efficiency is still limited. The electronic band gap of conventional TiO_2 is in UV region whose intensity accounts for approximately 5 % of total energy from solar spectrum [2]. According to this viewpoint, TiO_2 has been modified by various methods to expand its photoresponse into visible region, which is the major component of solar spectrum. The modification methods can be categorized into three generations. The first generation involves the use of pure TiO_2 , the second is the use of metal doped TiO_2 , and the third involves with non-metal doped TiO_2 [3, 4]. Doping TiO_2 with metals can reduce the band gap energy, resulting in the absorption band shifted to the visible region; furthermore, metal dopants can bring down the electron–hole recombination rate. Similar effects are attained with non-metal doped TiO_2 [5, 6]. On account of these advantages, the modification of TiO_2 by co-doping with metal and nonmetal ions is a noteworthy approach for improving the efficiency of TiO_2 . The cooperative action can enhance the photocatalytic activity of TiO_2 . Recently, a number of research groups have reported various types of co-doped TiO_2 materials; and one of the most interesting co-doping couples is nitrogen and iron. Cong et al. [7] suggested that N and Fe incorporating in TiO_2 could expand the absorption edge to visible region; therefore, N–Fe– TiO_2 exhibited greater photo-efficiency for degradation of rhodamine B than that of undoped TiO_2 . Hao et al. [8] synthesized mesoporous TiO_2 co-doped with N and Fe^{3+} and reported that dodecylamine could act not only as a nitrogen source but also as a structure directing agent. The co-doped samples had better activity for photodegradation of 2,4-dichlorophenol under visible light than nitrogen doped TiO_2 and commercial grade TiO_2 (P25) samples.

In this paper, we prepared N and Fe co-doped TiO_2 nanocrystalline samples via a modified sol–gel method using dodecylamine as both nitrogen source and structure directing agent. These samples were characterized and tested for photocatalytic activity towards decomposition of methyl orange dye.

Experimental

A desired amount of $\text{Fe}(\text{NO}_3)_3 \cdot 9\text{H}_2\text{O}$ was dissolved in 45 mL of 1.8 M HNO_3 aqueous solution. Then, 10 mL of $\text{Ti}(\text{O}i\text{Bu})_4$ was added into the solution mixture with vigorous stirring. After precipitate was formed, the mixture was refluxed at 80 °C for 2 h. Followed by an addition of 3.37 mL of dodecylamine (DDA) and the resulting sol was refluxed for another 30 min. Then, the sol was aged at 80 °C for 2 days. The white gel was dried at 80 °C for at least 1 day. The as-synthesized sample was subsequently calcined in air at 450 °C for 2 h with a heating rate of 1 °C/min. The synthesis of N– TiO_2 and undoped- TiO_2 can be achieved without $\text{Fe}(\text{NO}_3)_3 \cdot 9\text{H}_2\text{O}$ addition; and ethanol extraction was performed for undoped- TiO_2 .

Powder X-ray diffraction (XRD) data were collected using Bruker D8 ADVANCE diffractometer (Cu $K\alpha_1$ radiation with Ge-crystal (Johansson type)

monochromator ($\lambda = 1.540619 \text{ \AA}$). Functional groups of samples were determined by FT-IR spectroscopy (EX FT-IR system, Perkin Elmer Instrument) using KBr pellet. The UV-Vis absorption spectra were recorded on PerkinElmer Lambda 800 UV-Vis spectrometer, using BaSO_4 as a reflectance sample. The morphologies of the samples were examined by scanning electron microscopy (SEM); (15 kV, Hitachi S-2500) and transmission electron microscopy (TEM) (200 kV). The presence of Fe^{3+} in the samples was investigated by electron spin resonance (ESR) spectrometer (Elexsys E 500, Bruker) at 277 K; and the Fe content was determined by wavelength dispersive X-ray fluorescence (XRF) spectrometer (Bruker AXS model S4 Explorer equipped with Rh K radiation operating at 50 kV and 20 mA).

The photodegradation of methyl orange was carried out by using a home-made glass reactor with water cooling jacket. A 0.05 g of TiO_2 sample was suspended in 50 mL of methyl orange solution (30 ppm). After sonicated for 10 min, the reaction mixture was stirred in the dark for 60 min to attain the adsorption-desorption equilibrium for methyl orange solution and dissolve oxygen on the surface of TiO_2 . Subsequently, the obtained mixture was illuminated with UV (80-W mercury lamp) or visible light (500 W halogen lamp with a UV cut glass filter) under stirring. After every given irradiation time, an aliquot of sample was collected from the reaction mixture and centrifuged at 3,000 rpm for 20 min. The residual concentration of methyl orange solution was measured with a UV-Vis spectrophotometer (Genway20).

Results and discussion

Figure 1 shows XRD patterns of undoped- TiO_2 , N- TiO_2 and N-0.1 %Fe- TiO_2 samples compared to that of commercial TiO_2 (P25). All synthesized TiO_2 samples consist of anatase phase structure mixed with rutile, in contrast to the results reported by Hao et al. [8], where anatase and brookite phases were detected. Although DDA was used in the synthesis for both cases, the different crystalline phases of the obtained TiO_2 samples signify the influence of preparation conditions (e.g., reaction temperature and time, precursor concentration, and calcination condition) on the resulting TiO_2 structure. For N-Fe- TiO_2 sample, neither iron oxide nor Fe_xTiO_y crystalline phases were observed in the XRD pattern. These results indicate that iron ions are well dispersed into TiO_2 lattice. The average crystallite sizes of the samples were calculated using Debye-Scherrer equation and are summarized in Table 1. The crystallite size of N-Fe- TiO_2 sample is larger than those of N- TiO_2 and undoped- TiO_2 , illustrating the beneficial effect of iron dopant on crystal growth [7, 8]. In addition, hydroxyl and amine functional groups were detected in the FT-IR spectra of N- TiO_2 and N-Fe- TiO_2 samples. Hydroxyl groups are common on surface of metal oxide. However, the presence of amine groups suggests incomplete decomposition of DDA during calcination and some amine residues deposited on TiO_2 surface. The Fe-O-Ti vibration was not observed in the FT-IR spectrum of N-Fe- TiO_2 sample; however, the presence of Fe content was determined by XRF technique to be 0.1 wt %, which is corresponded to the amount added to the synthetic mixture.

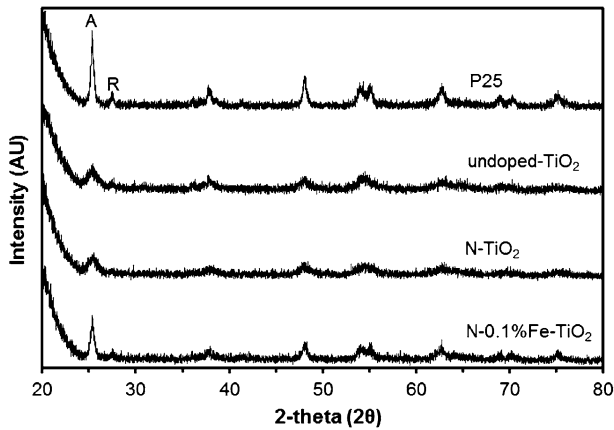


Fig. 1 XRD patterns of undoped-TiO₂, N-TiO₂, N-0.1 %Fe-TiO₂ and P25 (A anatase, R rutile)

Table 1 Structural phases, average crystallite sizes, and energy band gaps of the synthesized TiO₂ and P25 samples

Samples	Phase	Crystallite size (nm)	Energy band gap (eV)
P25	Anatase/rutile	25.1	2.99
Undoped-TiO ₂	Anatase/rutile	6.2	2.89
N-TiO ₂	Anatase/rutile	10.5	2.94
N-0.1 %Fe-TiO ₂	Anatase/rutile	18.2	2.92

Morphologies of the synthesized TiO₂ samples were examined by SEM and TEM (Fig. 2). The SEM images show rough surface and particle agglomeration for all samples. The TEM images reveal that the primary particle size and shape of all synthesized TiO₂ samples are very similar with an average particle size of ~ 7 nm.

Diffuse reflectance UV-Vis spectra of the synthesized TiO₂ samples show absorption edges in the range of 405–420 nm (Fig. 3). Compared to that of the commercial grade TiO₂ (P25, Degussa), the absorption spectra of the synthesized TiO₂ do not clearly show an extended red shift. Among the samples studied, the highest absorption edge is, surprisingly, belong to undoped-TiO₂, at ~ 420 nm, and P25 TiO₂ exhibits an absorption edge at the shortest wavelength of 405 nm. The energy band gaps of all samples were calculated from the adsorption edge and are shown in Table 1.

ESR experiment was carried out for Fe³⁺ detection in the samples and the spectra are shown in Fig. 4. The signal centered at $g \approx 2.00$ was only observed for N-Fe-TiO₂ samples and assigned to Fe³⁺ spin ($S = 5/2$) in octahedral symmetry of anatase due to Fe³⁺ substituted for Ti⁴⁺ in TiO₂ lattice [9]. According to ESR signals (not shown here), the increasing in Fe³⁺ dopant concentration brought about an increase in the intensity of the paramagnetic signal. The presence of Fe³⁺ is further assured by the signal at $g \approx 4.22$, which is attributed to Fe³⁺ substituted in the lattice adjacent to a charge-compensating oxide anion vacancy [8, 10].

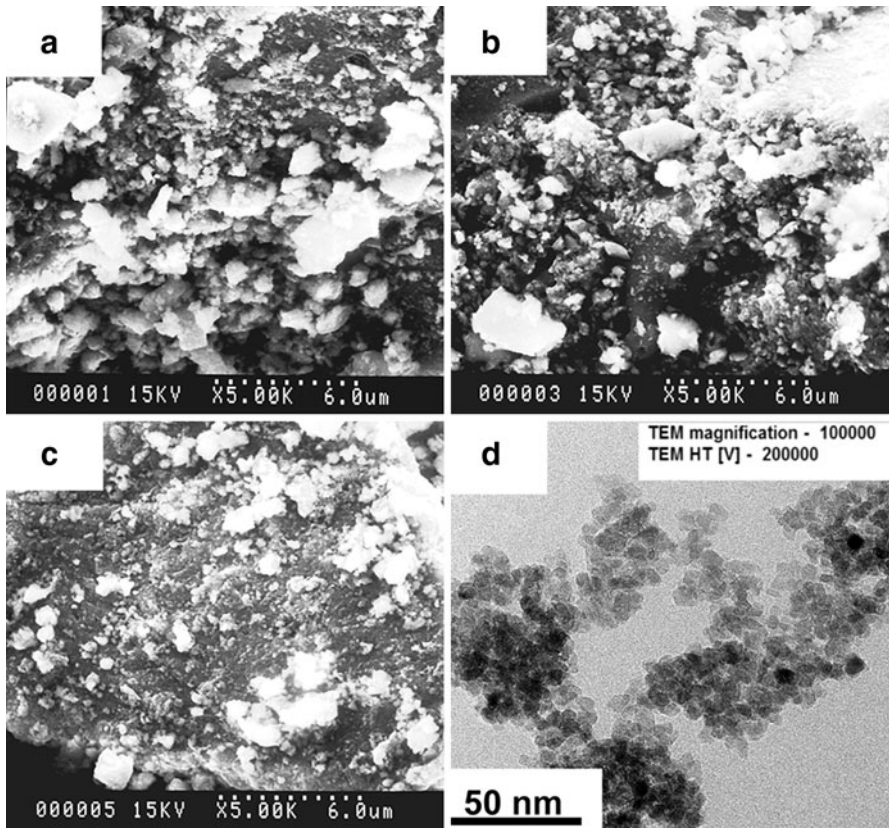


Fig. 2 SEM images of **a** undoped-TiO₂, **b** N-TiO₂, **c** N-0.1 %Fe-TiO₂, and **d** TEM image of N-TiO₂

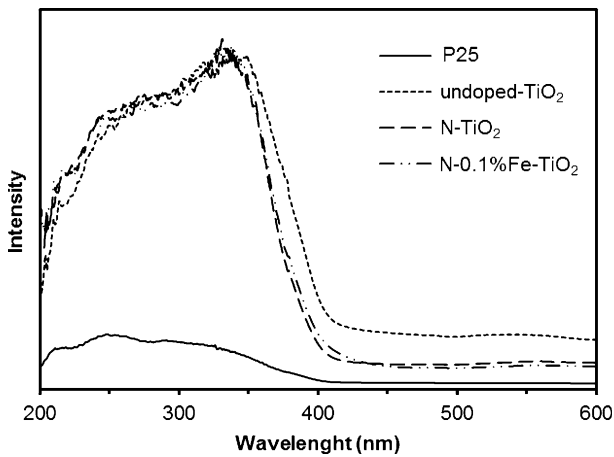


Fig. 3 UV-Vis spectra of P25, N-TiO₂, N-0.1 %Fe-TiO₂ and undoped-TiO₂

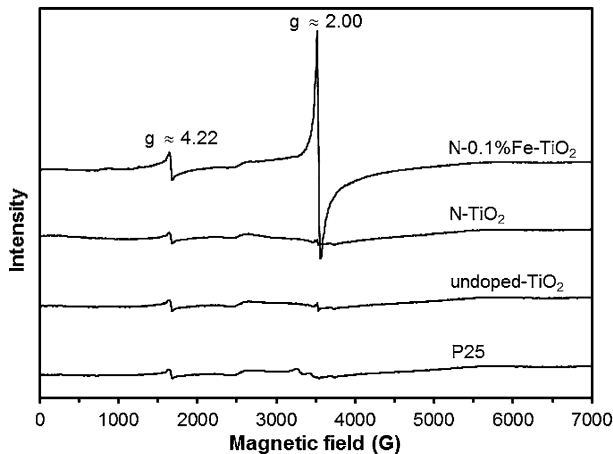


Fig. 4 EPR spectra of undoped-TiO₂, N-TiO₂, N-0.1 %Fe-TiO₂, and P25

The N doped, N-Fe co-doped and undoped TiO₂ samples were tested for their photocatalytic activity towards the degradation of methyl orange dye under 80 W UV lamp (Fig. 5). The concentration of methyl orange dye solution gradually decreased when time increased. The methyl orange dye was completely decomposed when the reaction was stirred under UV light irradiation overnight. However, the decomposition rate was greatest when P25 TiO₂ was used. The synthesized TiO₂ photocatalysts provided a similar but lower rate independent of the doping species. On the other hand, under a 500 W visible lamp, the methyl orange dye was not degraded. Thus, the synthesized TiO₂ samples are only photocatalytically active under UV light. These photocatalytic results are consistent with the UV-Vis absorption spectra where no clear red-shift was observed for N-TiO₂ and N-Fe-TiO₂ samples. The results were perhaps explained by the fact that the nitrogen

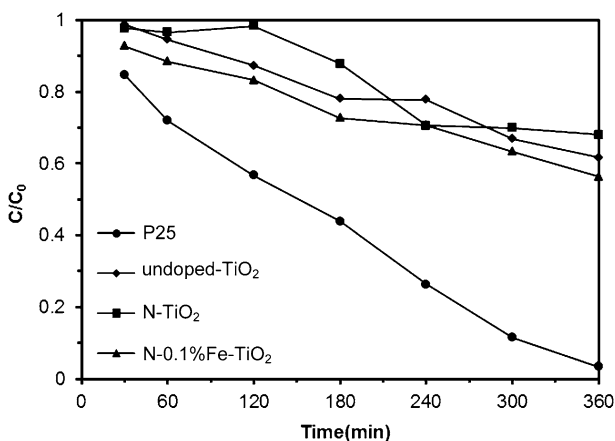


Fig. 5 The decomposition of 30 ppm methyl orange dye using P25, undoped-TiO₂, N-TiO₂ and N-0.1 %Fe-TiO₂ catalysts under 80 W UV lamp

content in the TiO₂ lattice is very low and too low to cause a shift in the absorption edge of the samples. In addition, the nitrogen species may only be present in the form of surface amine; as a result, no visible absorption was observed. The slightly higher degradation rate of N–Fe–TiO₂ sample compared to those of N–TiO₂ and undoped-TiO₂ samples is likely because of the existence of Fe³⁺ ion. The absorption spectra of all synthesized samples are similar; therefore, the higher photocatalytic activity of N–Fe–TiO₂ sample is resulted from the lower electron–hole recombination rate due to the presence of Fe³⁺ ion [8, 11].

Conclusions

The modified TiO₂ samples were successfully prepared via sol–gel method using dodecylamine (DDA) and Fe(NO₃)₃·9H₂O as N and Fe sources, respectively. The dopants improved crystallite size of the prepared TiO₂ samples; nonetheless, the morphologies of all TiO₂ samples were not different in size and appearance. The presence of Fe³⁺ dopant in the sample was confirmed by ESR technique. In addition, N doping and N–Fe co-doping did not lead to a significant shift of the absorption edge or change in energy band gap compared to those of the synthesized pure TiO₂ or commercial P25 Degussa samples. Corresponding with the absorption spectra, the synthesized TiO₂ samples show photocatalytic activity only under UV light irradiation, but not under visible light irradiation.

Acknowledgments This project is supported by the Office of the Higher Education Commission and Mahidol University under the National Research Universities Initiative. Financial support from the Thailand Research Fund (TRF) and the Center of Excellence for Innovation in Chemistry (PERCH-CIC), Commission on Higher Education, Ministry of Education are also gratefully acknowledged.

References

1. R.P.K. Wells, in *Met. Oxide Catal.*, vol. 2, ed. by S.D. Jackson, J.S.J. Hargreaves (Wiley-VCH, London, 2009), p. 756
2. H. Choi, E. Stathatos, D.D. Dionysiou, *Desalination* **202**, 199 (2007)
3. B. Naik, K.M. Parida, *Ind. Eng. Chem. Res.* **49**, 8339 (2010)
4. S. Bouattour, A.M.B.D. Rego, L.F.V. Ferreira, *Mater. Res. Bull.* **45**, 818 (2010)
5. C. Chem, W. Ma, J. Zhao, *Curr. Org. Chem.* **14**, 630 (2010)
6. J.J. Zou, B. Zhu, L. Wang, X. Zhang, Z. Mi, *J. Mol. Catal. A* **286**, 63 (2008)
7. Y. Cong, J. Zhang, F. Chen, M. Anpo, D. He, *J. Phys. Chem. C* **111**, 10618 (2007)
8. H. Hao, J. Zhang, *Microporous Mesoporous Mater.* **121**, 52 (2009)
9. J. Zhu, W. Zheng, B. He, J. Zhang, *J. Mol. Catal. A* **216**, 35 (2004)
10. T. Tong, J. Zhang, B. Tian, F. Chen, D. He, *J. Hazard. Mater.* **155**, 572 (2008)
11. F. Dong, H. Wang, Z. Wu, J. Qiu, *J. Colloid Interface Sci.* **343**, 200 (2010)